Viral Infection Depends on Host's Metabolism

Anastasios Marantos,[1,*] Kim Sneppen,[1] Stanley Brown[1] and Namiko Mitarai[1]

[1]Niels Bohr Institute, University of Copenhagen, Blegdamsvej 17-21, 2100 Copenhagen Ø, Denmark.
[*]Corresponding author: anmaran@protonmail.com

Abstract

Phage infection begins with physical interaction and host cell entry, occurring through various strategies including exploitation of surface receptors, pili, or porins. Research has predominantly emphasized structural compatibility between phage and host, particularly attachment and recognition mechanisms. However, one critical layer remains underexplored: how host physiological state, particularly metabolic activity, influences entry likelihood. Here, we quantitatively compared phage adsorption efficiencies across diverse *Escherichia coli* phages under controlled metabolic conditions. Using a standardized protocol, we measured adsorption rates (η) for five phages representing various life cycles (lytic, lysogenic, chronic) and entry pathways (LamB, FhuA, pilus, Tsx). Four of the five phages exhibited significantly reduced commitment to infection under energy-limited conditions. Notably, this effect varied. Phages with high baseline η were less sensitive to metabolic inhibition than phages with low baseline η. This observation suggests weak-binding phages may disengage under unfavorable conditions to avoid non-productive infections. Our findings support a two-step infection model, where host energy availability modulates the transition from reversible binding to irreversible commitment to infection. Our study highlights the importance of considering host physiology when studying virus-host dynamics, especially in energy-limited environments.

Key words: phage, bacteria, *Escherichia coli*, adsorption, infection, metabolism

Introduction

Bacteriophages (phages) are viruses that infect bacteria, first identified by Frederick Twort and Félix d'Hérelle in the early 20th century [1, 2, 3]. To establish infection, phages must first encounter their host [4, 5] and then their genomes must successfully enter the bacterial cell [6, 7, 8, 9, 10, 11]. This process exploits bacterial surface structures such as outer membrane receptors, pili, and porins [12]. Phage-bacteria interactions are typically studied under controlled laboratory conditions [13]; however, in natural environments, bacteria often experience suboptimal conditions for growth, such as nutrient limitation, fluctuating temperatures, and variable energy availability [14]. These conditions profoundly influence host physiology [14] and exert strong eco-evolutionary pressures that shape phage-bacteria interactions and, by extension, microbial ecosystem dynamics [15, 16, 17, 18]. A critical factor in microbial life under suboptimal conditions is the impact on host metabolic activity. While the effects of metabolism on post-infection processes, such as viral replication and lysogeny, have been extensively studied [19, 20, 21, 22, 23, 24, 25, 26, 27, 28, 29, 30, 31, 32, 33, 34], its effect on viral adsorption has not received the same level of attention [35, 36].

The foundations of phage adsorption studies were set by the works of Krueger, Schlesinger, Luria, Delbrück and Weidel [37, 38, 39, 40, 41, 42, 43]. First hypothesized by Anderson and later experimentally demonstrated for the first time by Garen and Puck for phage T1, viral entry occurs in two distinct steps: an initial, reversible attachment that does not require energy, followed by an irreversible, energy-dependent binding step [44, 45, 46]. This mechanism was later corroborated and extended through the Institute Pasteur group's seminal studies on phage λ and its interaction with the LamB protein receptor [47, 48, 49, 50, 51, 52], as well as Volkmar Braun et al.'s pioneering work on the FhuA protein receptor, which serves as the entry point for phages T1, T5, and ϕ80 [53, 54, 55, 56, 57, 58, 59, 60, 61, 62, 63]. This two-step process exhibits interesting mechanistic nuances. Braun's research established that FhuA functions as a gated channel requiring energy for phage entry [58, 59, 60, 61]. While T1 and ϕ80 adsorption depend on host metabolism [55, 57], T5 can still enter energy-depleted cells [56, 57, 59]. This is because FhuA acts as a closed gate for the virus, requiring energy to undergo a conformational change that allows entry [56, 58, 60]. In energy-depleted cells, this energy-dependent conformational change does not occur, preventing most phages from entering. However, the closure of the FhuA channel is not absolute, and T5 manages to enter [56, 57, 59]. Notably, we observed that for phage λ, adsorption is also sensitive to the metabolic state of the host [64] and is inhibited by the same compounds that block LamB hyperdiffusion [65]. Moreover, a mutant phage variant (λh) could bypass this dependency, indicating that adsorption by wild-type λ is not solely determined by receptor presence but is also modulated by host energy availability in a non-trivial way. Furthermore, recent single-cell observations showed that phage entry probability decreases when the multiplicity of infection is high, due to changes in membrane integrity and loss of membrane potential [66]. Note that these energy dependences of phage adsorption are beyond what could be explained by bacteria cell size variation due to growth conditions [24].

Although these studies have independently explored the influence of host metabolism on phage adsorption, the phenomenon was rarely a central focus and often emerged as a secondary or incidental observation. This may partly explain why it has not yet received broader attention within the microbial ecology and microbiology communities [35, 36],

especially considering its implications for population-level virus–host interactions in environments where energy-limited conditions are the norm [14].

Here, we aim to bring this phenomenon back into focus by providing, for the first time to our knowledge, a systematic and quantitative comparison across different phages and entry pathways to test the generality and comparative effect of host's metabolism on viral adsorption. In this study, we investigated how the host's metabolic state influences bacteriophage entry efficiency across a diverse set of *E. coli* phages with different life cycles and entry mechanisms. By utilizing a common standardized experimental protocol, we provided a direct comparative analysis of adsorption efficiencies under identical conditions and quantified the dependence of phage adsorption rates on host metabolic state.

Our results demonstrate that metabolic-state-dependent entry is a widespread phenomenon, observed in four out of the five phages studied. This holds true across phages with diverse infection strategies, including lytic, lysogenic, and chronic phages, and entry pathways as diverse as LamB and FhuA receptors, the bacterial pilus, and the Tsx porin. To enable direct quantitative comparisons, we measured the adsorption rate constant (η) for each phage under standardized conditions, providing one of the few comparative accounts of η across multiple phages. We further quantified how host metabolism affects adsorption efficiency and found a strong correlation: phages with higher baseline η values under energy-rich conditions were less sensitive to metabolic inhibition. This suggests that phages with strong-binding strategies are more committed to infection and less influenced by host metabolic fluctuations, whereas weak-binding phages may have evolved to limit entry under unfavorable conditions, thereby reducing the likelihood of non-productive infections.

Materials and Methods

This experiment examined phage adsorption to *Escherichia coli* cells under two contrasting metabolic states: a state of high metabolic activity due to the presence of glucose, and a state of low metabolic activity due to the presence of potassium arsenate and sodium azide. The following protocol was adapted from the experimental methodology of the study by Brown et al. [64] (see Fig. 1 and Supplementary Information for greater detail).

Each bacterial culture was initiated from an independent single colony, and each phage lysate was prepared from an independent plaque. Following overnight growth, the bacterial culture was diluted 20-fold in rich medium and incubated for 2 hours to restore exponential growth. Subsequently, nutrients were removed from the bacteria through repeated centrifugation and resuspension in a nutrient-free buffer.

After washing, the samples of the washed bacteria were subjected to favorable or unfavorable growth conditions by adding glucose and potassium phosphate or potassium arsenate and sodium azide, respectively, and incubating at 37 °C for 10 minutes. Post incubation, phages were introduced at a low multiplicity of infection (MOI), on the order of 0.001, to reduce the likelihood of coinfections and incubation continued. We allowed sufficient time for phage infection but not for lysis, to ensure that only first-generation viruses were present. As a result, the incubation time varied for each strain, as our goal was to maximize the incubation period while being limited by the need to complete manipulations before the first infection cycle was completed. The free phages were then separated from the bacteria by centrifugation. A portion of the supernatant was subsequently diluted 10-fold with buffer, supplemented with potassium phosphate to neutralize any residual arsenate toxicity. Phage titers were assessed by serial dilutions in buffer and spotted on a lawn of a susceptible bacterial strain. The concentration of washed bacteria was estimated by turbidity at 600nm. The turbidity was calibrated with a Petroff-Hausser chamber. The proportion of unbound phage was calculated by comparing the concentration as PFU/ml in the supernatant derived from bacteria-containing samples with that of bacteria-free samples.

To ensure robust control conditions, parallel experiments were conducted under various configurations. These included: (i) samples containing bacteria resistant to phages, (ii) samples containing only phages, with no bacteria present, (iii) samples containing only bacteria, with no phages, and (iv) samples containing neither phages nor bacteria, with only buffer. These controls allowed us to account for background effects and isolate the specific interactions between phages and sensitive bacterial populations. To accurately quantify viral entry efficiency, we used isogenic pairs for our permissive-resistant host controls.

Results

To assess the impact of the host's metabolic state on viral entry, we exposed each phage to bacteria under both energy-competent and energy-depleted conditions, as described in *Materials and Methods*. By titering the viral particles in the post-cellular supernatant and comparing permissive hosts to resistant hosts and buffer controls under each condition, we quantified entry efficiency for each metabolic state (as shown in Tables S1 and S2).

To quantify the effect, we calculated the ratios of free viruses from permissive (R_P) and resistant hosts (R_R) respectively, to the free viruses in the buffer under energy-depleted (As/Az) and energy-competent (Glu) conditions. Our primary metric of interest is the ratio of these ratios, which we refer to simply as the "Ratio". This metric captures the relative change in viral commitment to infection between high and low metabolic state conditions. It is defined as:

$$\begin{aligned}\text{Ratio} &= \frac{\text{Free viruses in As/Az}}{\text{Free viruses in Glu}} \\ &= \frac{\left(\dfrac{\text{Viral particles in Arsenate and Azide}}{\text{Viral particles in Buffer}}\right)}{\left(\dfrac{\text{Viral particles in Glucose}}{\text{Viral particles in Buffer}}\right)}\end{aligned}$$

with "Free viruses in As/Az" and "Free viruses in Glu" being either R_P or R_R (see Tables S1 and S2) depending on the bacteria under study.

The results of these experiments are visualized in Fig. 2 and detailed in the lower half of Tables S1 and S2. If there were no effect of metabolic state on viral entry, as seen in the resistant control case, the Ratio in the permissive strains case would be equal to 1. However, we observe that this is not the case for phages λ, ϕ80, m13, and T6 (Figs. 2A-D, where the Ratio is significantly greater than 1.

For the temperate lambdoid phages, λ and ϕ80, we observed an increase in free viruses of approximately 9.3 and 2.7 times, respectively (Figs. 2 A and 2 B). In the case of chronic bacteriophage m13, we see a greater than 3 times increase in viral particles when trying to infect an energy-depleted host

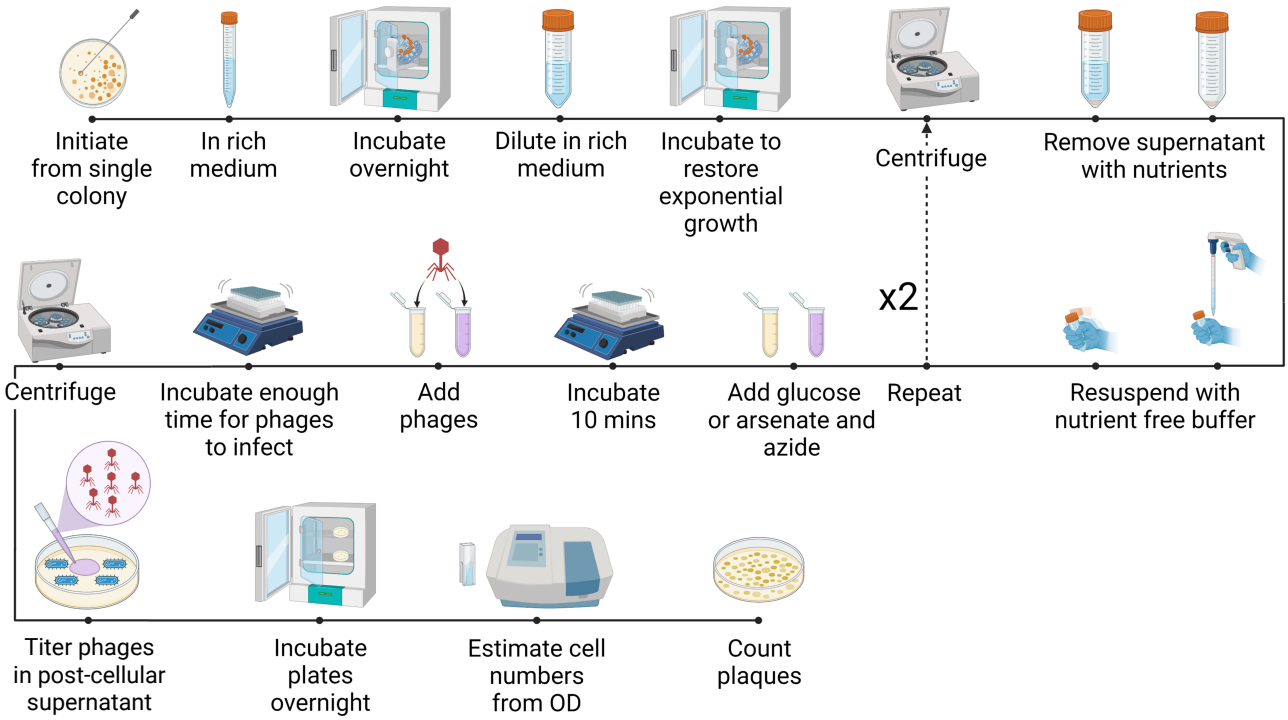

Fig. 1. The experimental protocol. Each dot represents a step in the experimental protocol. The accompanying text below and the image above provide a detailed description of the process. The sequence of steps follows the solid line from the upper left (start) to the lower right (end), indicating the correct order. The dotted line with an arrow and the "x2" marker denotes a looped process in the protocol. (Created in BioRender. Marantos, A. (2025) https://BioRender.com/2u4x65f.)

(Fig. 2 C) and for virulent bacteriophage T6, we observe an average ratio of around 1.6 (Fig. 2D). However, this effect does not appear to be universal, as for phage T5, the ratio remains equal to 1 (Fig. 2E).

It is important to note that the ratio measure is not directly comparable between different phages. As described in the *Methods and Materials* section, the incubation time varied for each phage strain (displayed in the top right corner of each panel in Fig. 2). This variation was necessary to maximize the incubation period while ensuring that manipulations were completed before the first infection cycle concluded. By allowing sufficient time for phage adsorption but preventing lysis, we ensured that only first-generation viruses were present. However, to make the effect of the host's metabolic state comparable across different phages, we need to eliminate the influence of time dependency.

To achieve this, we employed a standard mass-action kinetics model of phage adsorption [37, 38, 67, 39], where free viruses are removed from the medium through probabilistic random encounters with bacteria at a rate proportional to their concentration:

$$\frac{\mathrm{dP}}{\mathrm{dt}} = -\eta \mathrm{BP} \quad \Leftrightarrow \quad \mathrm{P(t)} = \mathrm{P(0)} \cdot \exp(-\eta \mathrm{Bt}),$$

where $\mathrm{B} = (3 \pm 0.5) \times 10^9$ cells/mL represents the bacterial density, assumed to remain constant throughout the relevant experimental period, as bacterial growth and lysis were negligible. Here, P(0) represents the initial viral concentration in the buffer, while P(t) corresponds to the viral concentration at a given time (see also Fig. S3). Therefore, the only factor differentiating the number of "Viral particles in Glucose" ($\mathrm{P_{GLU}(t)}$) and "Viral particles in Arsenate and Azide" ($\mathrm{P_{As/Az}(t)}$) for each phage is the adsorption rate, which we can now determine by solving for η:

$$\eta = -\frac{\ln[(\mathrm{P(t)/P(0)})]}{\mathrm{B} \cdot \mathrm{t_{phage}}} = -\frac{\ln[\mathrm{R_P}]}{\mathrm{B} \cdot \mathrm{t_{phage}}}, \tag{1}$$

where $\mathrm{t_{phage}}$ denotes the incubation time allowed for each respective phage.

Crucially, this approach also allows us to compare the effect of different metabolic conditions on adsorption across different phages, as this measure is now independent of the duration of time over which we measure phage adsorption. Defining η' as the adsorption rate in arsenate and azide, we can express the relative change in adsorption as:

$$\frac{\eta'}{\eta} = \frac{-\ln \mathrm{R_{P,\,As/Az}}/(\mathrm{Bt_{phage}})}{-\ln \mathrm{R_{P,\,Glu}}/(\mathrm{Bt_{phage}})} \quad \Leftrightarrow \quad \frac{\eta'}{\eta} = \frac{\ln \mathrm{R_{P,\,As/Az}}}{\ln \mathrm{R_{P,\,Glu}}}.$$

The results for each phage are summarized in Table 1, and analyzed in more detail in Table S2. The adsorption rates (η) were determined for each phage in glucose-grown cultures and compared with a range of adsorption rate values from the literature. While these comparisons provide useful context, caution is necessary, as differences in methodology, including experimental setup, bacterial and phage strains, and culturing conditions, can substantially influence adsorption rates. Such methodological variations have been shown to alter adsorption rates by an order of magnitude or more and occasionally even exceed a 100-fold difference [68, 69, 62, 70, 71]. For example, in the case of T6, where we observe the largest discrepancy, literature values were obtained using different bacterial strains,

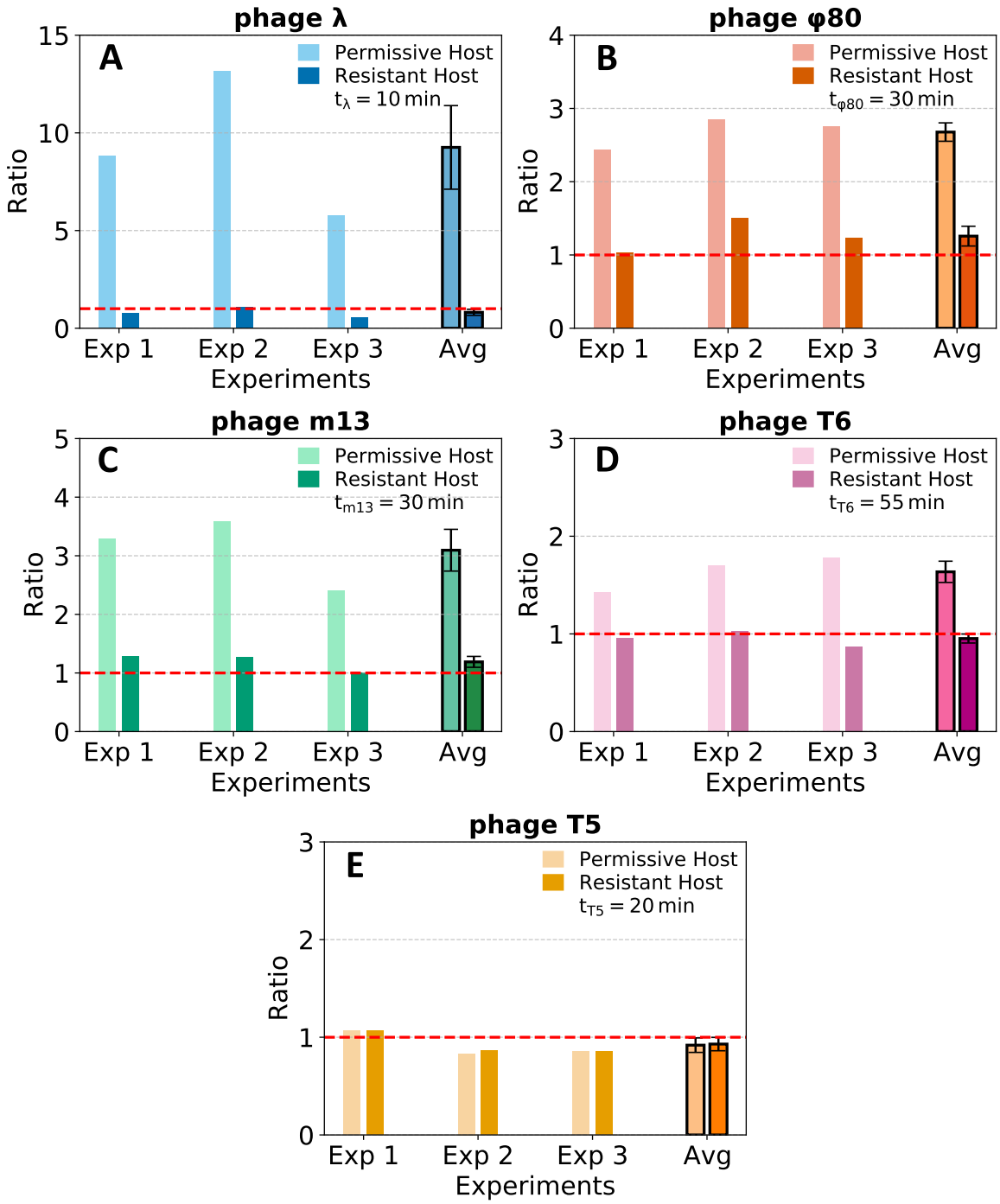

Fig. 2. Effect of hosts' metabolic condition on viral entry. Panels **A–E** display the results of the Ratio, defined as Ratio $= \frac{\text{Free viruses in AsAz}}{\text{Free viruses in Glu}} = \left(\frac{\text{Viral particles in Arsenate and Azide}}{\text{Viral particles in Buffer}}\right) / \left(\frac{\text{Viral particles in Glucose}}{\text{Viral particles in Buffer}}\right)$, for each of the three experiments and their average. Each panel corresponds to a specific phage, as indicated above the respective panel. Lighter-colored bars represent data from permissive hosts, while darker-colored bars show results from resistant host controls for comparison. The red horizontal dashed line represents the scenario where Ratio = 1, indicating that the number of free viral particles is the same in energy-competent and energy-depleted bacteria. The incubation time for each phage-host pair is consistent across all three experiments and is displayed in the upper-right corner of each panel.

media composition, and a significantly lower experimental temperature (24°C compared to our 37°C).

For all phages tested, the relative adsorption rate (η'/η) under arsenate and azide (As/Az) conditions indicated a reduction in adsorption efficiency. In the cases of m13 and T6, this effect was especially pronounced, with SEMs for η'/η exceeding the mean values. This variability arises from extremely low adsorption under As/Az conditions, where the number of free viral particles in the supernatant approached those of the buffer control (see Fig. S1 and Table S2).

Phage	η ($\times 10^{-11}$ mL/(CFU·min))	η'/η	Literature η ($\times 10^{-11}$ mL/(CFU·min))	Reference
λ	15.5 ± 2.7	0.53 ± 0.03	[1.3, 1100]	[72, 73, 69, 74, 70]
ϕ80	1.7 ± 0.3	0.37 ± 0.05	[11, 38]	[57, 73]
m13	1.32 ± 0.23	0.06 ± 0.08	[3, 9]	[75, 73]
T6	0.32 ± 0.06	0.08 ± 0.11	[93, 340]	[70]
T5	5.8 ± 1.2	1.03 ± 0.16	[4, 2500]	[68, 57, 73, 70]

Table 1. Adsorption rate in glucose (η) and the effect of altered metabolic conditions (growth in arsenate and azide) on it (η'/η) for different phages. This table presents the experimentally determined adsorption rates (η) for each phage when grown in glucose, along with the relative adsorption rates (η'/η) under arsenate and azide (As/Az) conditions, reflecting the impact of altered metabolic states. In the cases of m13 and T6, the relative adsorption rate (η'/η) exhibits increased variability, with SEMs exceeding the mean values. This is due to very low adsorption under As/Az conditions, where free viral particle counts approach those of the buffer control (see Fig. S1 and Table S2). While this inflates relative variability, the results remain consistent with a strong reduction in adsorption efficiency. Furthermore, corresponding literature value ranges for η are included for comparison, with references provided. However, it is important to highlight that such comparisons are limited by differences in experimental protocols, host and virus strains, and growth conditions (e.g., temperature and media). Altering any of these factors has been reported to cause variations in adsorption rates, typically by up to an order of magnitude, and in some cases by even more than a 100-fold [68, 69, 62, 70, 71]. For example, in the case of T6, where we observe the largest discrepancy, literature values were obtained using different bacterial strains, grown in different media, at 24°C, which is 13°C lower than the 37°C temperature used in our experiments.

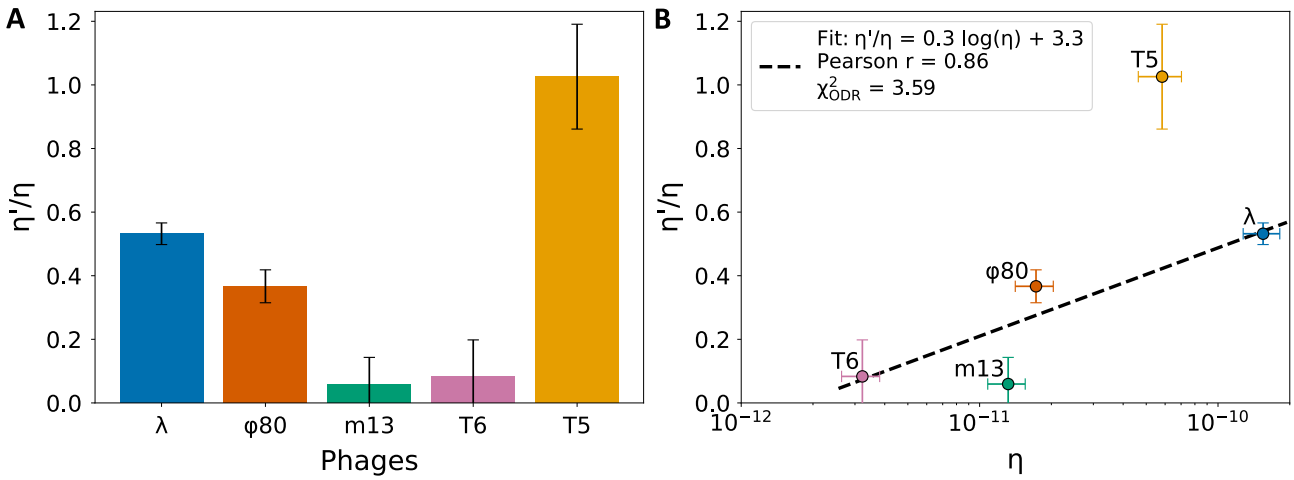

Fig. 3. Comparing the metabolic condition effect on phage adsorption rate. The y-axis of both panels represents the relative effect of growth in arsenate and azide (low metabolic condition) on the adsorption rate, η', compared to the adsorption rate in the high metabolic condition, η, for hosts grown in glucose. Panel **A** displays this effect for each phage (x-axis), while panel **B** illustrates the relationship between the effect and the adsorption rate in glucose, η. The dashed line represents a fitted model on the metabolic state sensitive phages that examines and quantifies the correlation between η'/η and η.

Despite this, the trend remains consistent with a substantial impairment of adsorption efficiency under metabolic stress.

Furthermore, in Fig. 3, we visualize the impact of metabolic conditions on adsorption rate across different phages. In panel A, we compare the ratio η'/η for each phage, while in panel B, we examine the relationship between metabolic condition sensitivity (η'/η) and the baseline adsorption rate in glucose (η) of each phage. In particular, among phages that exhibit metabolic state sensitivity, we observe a significant correlation between η'/η and $\log(\eta)$, with a Pearson correlation coefficient of $r = 0.86$, although with $r^2 = 0.74$ and an orthogonal distance regression fit that yields $\chi^2_{\text{ODR}} = 3.59$.

Discussion

We sought to determine whether the efficiency of viral entry is modulated by the metabolic state of the bacterial host. In the process we explored the generality of this phenomenon in a quantitative way that would allow for comparison between different phages. To address this, we exposed a diverse set of *E. coli* phages to bacterial cells under contrasting energy conditions and quantified the proportion of phages that failed to bind irreversibly to energy-depleted hosts, while retaining the ability to infect newly introduced hosts in an energy-competent state. Specifically, we measured the concentration of free phage particles remaining in the supernatant after a controlled adsorption period, using plaque assays to estimate the number of plaque-forming units (PFUs). Because only unadsorbed phages remain in the supernatant at this stage, and since the entire assay is completed before lysis, the PFU count

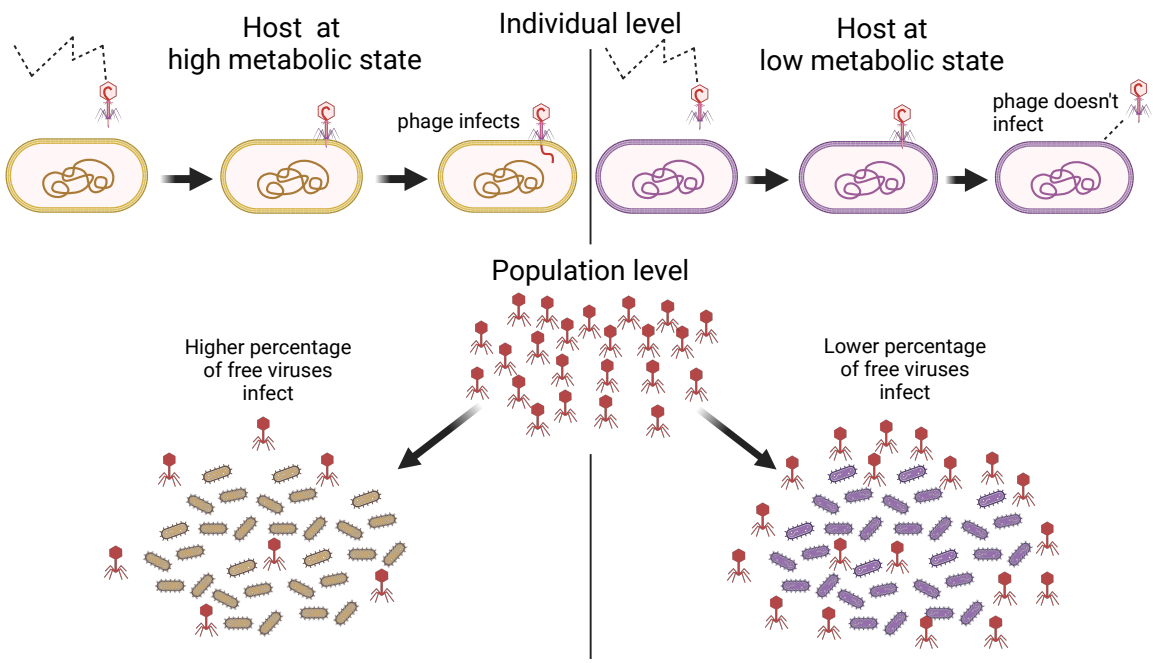

Fig. 4. Schematic of the Phenomenon. This illustration compares the ability of viral particles to enter upon encountering energy-competent bacteria (yellow, left) versus energy-depleted bacteria (purple, right). The upper part depicts a sequence of events, following the arrows from left to right, showing phage behavior when encountering a high-metabolic-state (energy-competent) host versus a low-metabolic-state (energy-depleted) host. At the population level, a greater percentage of free viral particles in the buffer will commit to infecting a community of high-metabolic-state hosts (grown in glucose) compared to those at a low metabolic state (grown in arsenate and azide).(Created in BioRender. Marantos, A. (2025) https://BioRender.com/3ymwbkk).

serves as a proxy for binding efficiency. By comparing PFU counts across energy-competent and energy-depleted conditions and normalizing them against buffer and resistant host controls, we quantified the extent to which entry depends on host metabolic activity.

This behavior is further illustrated in the schematics provided in Fig. 4, which summarizes the observed phenomenon. At the individual level, a phage moves through the environment in a random walk until it encounters a host. Our results reveal that if the host is in a high metabolic state, viral commitment occurs. In contrast, when the bacterium is in a low metabolic state, the phage does not bind irreversibly to the host. At the population level, this metabolic-state-dependent infection results in a higher proportion of free viral particles when bacteria are grown in conditions that induce low metabolic activity (e.g., arsenate or azide) compared to bacteria grown in glucose, which supports higher metabolic activity. Thus, the fraction of phages committing to infection is greater when encountering energy-competent hosts than when encountering energy-depleted hosts.

Further, by estimating the phage-specific adsorption rate constants (η), we corrected for differences in incubation time, enabling time-independent comparison across phage types. Our approach employs a simple, reproducible, and quantifiable framework in which all phages are studied in the same laboratory under consistent protocols, yielding directly comparable results across different viruses. The phenomenon exhibits remarkable generality, manifested across a variety of viral types, from lysogenic lambdoid phages (λ and ϕ80), to chronic phages (m13), and virulent phages (T6). Furthermore, these phages utilize distinct entry pathways to exploit the host. For instance, phage λ relies on the maltose uptake pathway through LamB [47], ϕ80 uses the iron uptake pathway through FhuA and TonB [54, 55, 57, 76], T6 exploits the Tsx porin [77, 78, 79, 80, 81], and m13 utilizes the pilus [75, 13].

Interestingly, despite this generality, the phenomenon does not apply to all phages. T5 does not exhibit dependence on the metabolic state of the host for entry, even though it also utilizes FhuA as its entry receptor [53, 82, 54, 56, 76], similar to ϕ80 [57, 83, 59, 60]. This is consistent with the findings of Braun et al., who showed that the differential behavior of ϕ80 and T5 can be attributed to their reliance (or lack thereof) on the FhuA–TonB energy transduction system [55, 56, 57, 59, 60]. TonB is part of the host's machinery for the uptake of ferrichromes and other compounds [84, 85, 86] and is required to energize FhuA during phage entry in the case of ϕ80 and T1 [55, 57, 59, 60]. However, T5 circumvents this requirement [56]. This suggests that in energy-depleted cells, where TonB function is compromised, phages dependent on TonB cannot trigger the conformational changes required to transition from reversible binding to the irreversible, energy-dependent state and proceed with DNA injection [59, 60]. In contrast, phages such as T5, which bypass this gate, can infect unimpeded. It remains unclear whether viruses themselves possess metabolic state-sensing capabilities, but Braun et al.'s findings suggest that this modulation arises primarily from host physiology [62, 63].

In contrast, our findings suggest that phage λ is capable of sensing the metabolic state of its host [64]. These results are particularly relevant to the current study, as we used the same protocol and observed consistent behavior from phage λ. Importantly, our previous study [64], along with the experiments described in this work and the cited studies by the Institut Pasteur group and Moldovan et al. [47, 48,

49, 50, 51, 52, 69], used λwt (also known as λPaPa [72]). This is not the original λ isolated in 1951 [87] (also known as Ur-λ [72]), but a laboratory derivative that has lost its accessory tail fibers, resulting in a lower adsorption rate and, consequently, the formation of larger plaques [72]. In Table 1, the upper range of the η literature values for λ is set by Ur-λ ([600, 1100] $\times 10^{-11}$ mL min^{-1} [72, 70]), while the lower range corresponds to the λPaPa strain ([1.3, 990] $\times 10^{-11}$ mL min^{-1} [73, 69, 74]). Phage λ, which requires the LamB protein for recognition and entry, was found to rely on the metabolic state of the host. We interpreted this behavior through λ's reversible binding mechanism [49] and the role of LamB hyperdiffusion under energy-sufficient conditions [88, 65]. While wild-type λ relies on these hyperdiffusive properties for infection, we observed that a mutant variant, λ*h*, which does not depend on them, was able to infect even energy-depleted hosts. Furthermore, our data indicate that this phenomenon is not due to direct effects of arsenate or azide on phage physiology, as the mutant λ*h* remained unaffected by these treatments and could infect the host as if the conditions were glucose-rich.

Because arsenate and azide are well-established inhibitors of cellular energy metabolism, they serve as effective tools for studying this phenomenon. The fact that a mutation in the tail fiber of λ*h* disables the phage's ability to differentiate hosts based on metabolic state suggests that this sensitivity may be an evolved function. Interestingly, a wild-type virulent mutant λ was observed not to adsorb to purified LamB extracted from *E. coli* K-12 in Tris buffer, but binds to LamB purified from *Shigella* [48], indicating that the properties of host-encoded receptors may also influence whether a phage can detect host metabolic status. Such mechanistic insights are currently feasible only for phages like λ, whose infection cycles are relatively well understood. Nevertheless, λ serves as a valuable model for understanding a broader and generalizable phenomenon.

In addition to establishing the generality of this phenomenon, our study contributes one of the few comparative accounts of directly measured adsorption rate constants (η) under standardized conditions. These rates varied considerably across phages, and when comparing η under high and low metabolic states, we observed substantial variation in sensitivity. Notably, the degree of adsorption reduction under metabolic inhibition—captured by the ratio η'/η—was strongly correlated with the baseline adsorption rate in glucose-rich conditions. Phages with higher baseline η values (e.g., λ) were less sensitive to metabolic suppression, whereas those with lower adsorption rates (e.g., m13) were more affected. This relationship implies that phages capable of rapid and strong binding are more committed to infection, regardless of host state, while others may "sample" the host and disengage if conditions are suboptimal.

A two-step infection model with an error-correction mechanism offers a useful lens to understand the underlying process (see Fig. 5 and references [46, 51, 69]). In this framework, free phages P first bind reversibly to host cells B with a rate constant k, forming a transient bound complex $[BP]$. From this state, the phage either proceeds to inject its DNA at rate k_{inj}, completing the entry, or unbinds and returns to the free state with rate k_{off}.

Assuming that the bound state reaches a quasi-steady-state ($\frac{d[BP]}{dt} \approx 0$), the rate of formation of the bound complex is balanced by the combined rates of dissociation and infection:

$$k \cdot P \cdot B = (k_{\text{off}} + k_{\text{inj}}) \cdot [BP] \quad \Leftrightarrow \quad [BP] = \frac{k \cdot P \cdot B}{k_{\text{off}} + k_{\text{inj}}}$$

The rate of successful infection is determined by the number of complexes that proceed to irreversible DNA injection:

$$k_{\text{inj}}[BP] = \frac{k}{1 + k_{\text{off}}/k_{\text{inj}}} \cdot P \cdot B$$

This represents the rate at which free phages are irreversibly removed from the system. Considering a small time interval Δt, the fraction of phages lost is approximately:

$$\frac{\Delta P}{P} \approx \frac{k}{1 + \frac{k_{\text{off}}}{k_{\text{inj}}}} \cdot B \cdot \Delta t$$

Connecting this to our mass-action model kinetics of phage adsorption, we have:

$$\begin{aligned} \frac{dP}{dt} &= -\eta B P \\ \Rightarrow \quad \frac{\Delta P}{P} &\approx \eta B \Delta t \quad \text{(for small } \Delta t\text{)} \\ \Leftrightarrow \quad \eta B \Delta t &= \frac{k}{1 + \frac{k_{\text{off}}}{k_{\text{inj}}}} B \Delta t \\ \Leftrightarrow \quad \eta &= \frac{k}{1 + \frac{k_{\text{off}}}{k_{\text{inj}}}} < k \end{aligned}$$

This shows that the effective adsorption rate η is always lower than the initial encounter rate k due to the possibility of unbinding before commitment to infection. This indicates that k_{inj} is more sensitive to metabolic state than k_{off}, meaning that larger fraction of binding events lead to successful entry into active cells. In energy-depleted cells, however, k_{inj} can become much smaller ($k_{\text{inj}} \ll k_{\text{off}}$), effectively reducing the adsorption rate η'. This suggests that phages avoid committing to unsuccessful infections not by increasing the likelihood of unbinding, but by reducing the probability of irreversible entry.

The above model also allows us to understand the observed correlation between η and η'/η as a result of phages with relatively larger k_{off} versus the tight binding phages with small k_{off}. Phages with large k_{off} will have naturally small η even for active cells, implying that a substantial fraction of encounters do not result in successful entry.

These results support the idea that host physiology acts not only as a barrier but also as a selective filter that influences phage infection strategies. This aligns with our findings and suggests that phages may exploit host energy levels as an internal "checkpoint", committing to infection only when the host is in a metabolically favorable state. These infection "checkpoints" may represent an elegant evolutionary strategy to minimize non-productive infection. However, such a checkpoint mechanism entails a fitness cost as some phages may leave viable hosts, but likely helps avoid wasteful infection attempts in poor environments. Conversely, phages like T5, which readily infect metabolically inactive cells, may be better suited to ecological niches such as biofilms or stationary-phase populations where energy-limited cells dominate. This is consistent with previous findings that T5 can replicate in starved bacterial cells [89].

Together, our findings support the view that phage-host interactions are not solely determined by receptor compatibility

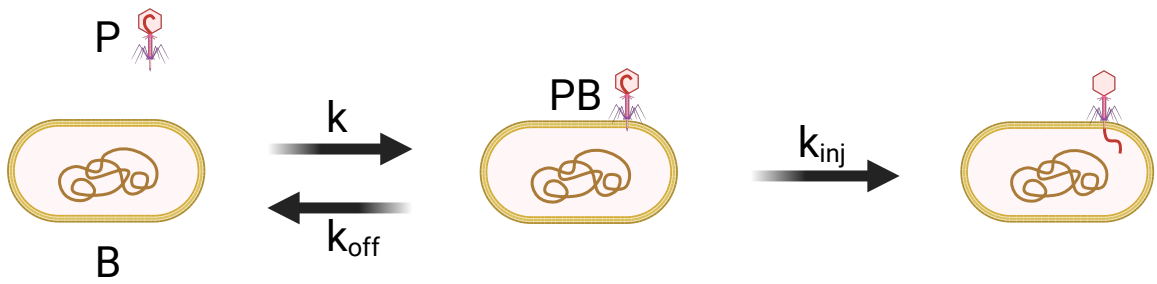

Fig. 5. 2-step infection dynamics with error-correction. The phage binds to its receptor but can leave again with a rate k_{off} as introduced in [46, 51, 69]. If bacteria are healthy, the phage injects easily with rate $k_{inj} \gg k_{off}$, and the infection rate is $\sim k$. The paper explores starved bacteria where some phages have a reduced injection rate $k_{inj} \ll k_{off}$ and an associated reduced adsorption rate η'. Compared to standard error correction, where the undesirable pathway is reduced by high k_{off}, the phage disfavors unfavorable infection by reducing k_{inj}. This check-point requires a finite k_{off}, implying a cost of some phages that leave a healthy host. (Created in BioRender. Marantos, A. (2025) https://BioRender.com/1mhwucl).

but are dynamically modulated by host physiology. Host energy availability emerges as a key determinant of infection success at the earliest stages of the viral life cycle. This insight may help explain variation in phage efficacy in natural and clinical settings, where bacterial populations exhibit substantial physiological heterogeneity [90, 91, 92, 93]. In conclusion, we provide direct evidence that viral entry efficiency is shaped by the metabolic condition of the bacterial host. This effect, while widespread, varies in magnitude and mechanism. By combining a unified experimental framework with adsorption kinetics modeling, we reveal a physiologically gated layer of phage infection that likely contributes to both ecological dynamics and evolutionary strategies. Our work underscores the importance of incorporating host physiology into models of viral infection, especially in contexts where metabolic diversity is the norm.

Data and code availability

The experimental data supporting the findings of this study are provided in the Supplementary Material. The code used for data analysis is available on GitHub at `https://github.com/TassosMar/Viral-Infection-Depends-on-Host-s-Metabolism.git`.

Competing interests

No competing interest is declared.

Author contributions statement

A.M. and S.B. conceived the study. Experiments were conducted by A.M. with assistance from S.B. and N.M. Data analysis was performed by A.M. under the guidance of N.M., K.S., and S.B. Modeling was conceived by N.M. and K.S. The project was supervised by K.S., S.B., and N.M. All authors contributed to writing, reviewing, and editing the manuscript. Funding was acquired by N.M. and K.S.

Acknowledgments

This research was funded by the Novo Nordisk Foundation (NNF21OC0068775) and the Danish National Research Foundation (grant number DNRF170). We thank Sine Lo Svenningsen and Adrien Sarlet for providing strains and Mireia Cordero for guidance in laboratory techniques.

References

1. Twort FW. An Investigation on the Nature of Ultra-Microscopic Viruses. *The Lancet*, 186(4814):1241–1243, 1915.
2. d'Hérelles F. Sur un microbe invisible antagoniste des bacilles dysentériques. *Comptes Rendus de l'Académie des Sciences de Paris*, 165:373–375, 1917. Archived (PDF) from the original on 11 May 2011. Retrieved 5 September 2010.
3. Keen EC. A century of phage research: bacteriophages and the shaping of modern biology. *BioEssays : news and reviews in molecular, cellular and developmental biology*, 37(1):6—9, 2015.
4. Adam G and Delbrück M. Reduction of dimensionality in biological diffusion processes. In A. Rich and N. Davidson, editors, *Structural Chemistry and Molecular Biology*, pages 198–215. W.H. Freeman & Company, San Francisco, 1968.
5. Berg HC and Purcell EM. Physics of chemoreception. *Biophysical Journal*, 20(2):193–219, 1977.
6. Tolmach LJ. Attachment and penetration of cells by viruses. volume 4 of *Advances in Virus Research*, pages 63–110. Academic Press, 1957.
7. Hu B, Margolin W, Molineux IJ, and Liu J. The bacteriophage t7 virion undergoes extensive structural remodeling during infection. *Science*, 339(6119):576–579, 2013. Epub 2013 Jan 10.
8. Bebeacua C, Tremblay D, Farenc C, Chapot-Chartier M-P, Sadovskaya I, van Heel M, Veesler D, Moineau S, and Cambillau C. Structure, adsorption to host, and infection mechanism of virulent lactococcal phage p2. *Journal of Virology*, 87(22):12302–12312, 2013. Epub 2013 Sep 11.
9. Spinelli S, Veesler D, Bebeacua C, and Cambillau C. Structures and host-adhesion mechanisms of lactococcal siphophages. *Frontiers in Microbiology*, 5:3, 2014. Epub 2014 Jan 16.
10. Rothenberg E, Sepúlveda LA, Skinner SO, Zeng L, Selvin PR, and Golding I. Single-virus tracking reveals a spatial receptor-dependent search mechanism. *Biophysical Journal*, 100(12):2875–2882, 2011.
11. Wedd C, Yunusov T, Smith A, Li R, Hardo G, Hunter M, Majed R, Fusco D, and Bakshi S. Single-cell imaging of the lytic phage life cycle in bacteria. *bioRxiv*, pages 2024–04, 2024.
12. Bertozzi Silva J, Storms Z, and Sauvageau D. Host receptors for bacteriophage adsorption. *FEMS Microbiology Letters*,

363(4):fnw002, February 2016. Epub 2016 Jan 10.
13. Madigan MT, Bender KS, Buckley DH, Sattley WM, and Stahl DA. *Brock Biology of Microorganisms*. Pearson Education, Inc., Boston, fifteenth edition, 2018.
14. Lennon JT and Jones SE. Microbial seed banks: the ecological and evolutionary implications of dormancy. *Nature Reviews Microbiology*, 9(2):119–130, 2011.
15. Jones SE and Lennon JT. Dormancy contributes to the maintenance of microbial diversity. *Proceedings of the National Academy of Sciences of the United States of America*, 2010.
16. Shoemaker WR and Lennon JT. Evolution with a seed bank: The population genetic consequences of microbial dormancy. *Evolutionary Applications*, 11(1):60–75, 2018.
17. Claudia I. Phenotypic flux: The role of physiology in explaining the conundrum of bacterial persistence amid phage attack. *Virus evolution*, 8(2):veac086, 2022.
18. Măgalie A, Marantos A, Schwartz DA, Marchi J, Lennon JT, and Weitz JS. Phage infection fronts trigger early sporulation and collective defense in bacterial populations. *bioRxiv*, 2024.
19. Kourilsky P. Lysogenization by bacteriophage lambda. II. Multiple infection and the lysogenic response. *Mol Gen Genet*, 122(2):183–195, 1973.
20. Kourilsky P. Lysogenization by bacteriophage lambda. II. Identification of genes involved in the multiplicity dependent processes. *Biochimie*, 56(11-12):1511–1516, 1974.
21. Kourilsky P and Knapp A. Lysogenization by bacteriophage lambda. III. Multiplicity dependent phenomena occurring upon infection by lambda. *Biochimie*, 56(11-12):1517–1523, 1974.
22. Kourilsky P and Gros D. Lysogenization by bacteriophage lambda. IV. Inhibition of phage DNA synthesis by the products of genes cII and cIII. *Biochimie*, 58(11-12):1321–1327, 1976.
23. Stewart FM and Levin BR. The population biology of bacterial viruses: why be temperate. *Theoretical Population Biology*, 26(1):93–117, 1984.
24. Hadas H, Einav M, Fishov I, and Zaritsky A. Bacteriophage t4 development depends on the physiology of its host *Escherichia coli*. *Microbiology (Reading, England)*, 143(Pt 1):179–185, 1997.
25. Arkin A, Ross J, and McAdams HH. Stochastic kinetic analysis of developmental pathway bifurcation in phage lambda-infected Escherichia coli cells. *Genetics*, 149(4):1633–1648, 1998.
26. You L, Suthers PF, and Yin J. Effects of *Escherichia coli* physiology on growth of phage t7 in vivo and in silico. *Journal of Bacteriology*, 184(7):1888–1894, 2002.
27. Ptashne M. *A Genetic Switch, Third Edition, Phage Lambda Revisited*. Cold Spring Harbor Laboratory Press, 2004.
28. Zeng L, Skinner SO, Zong C, Sippy J, Feiss M, and Golding I. Decision making at a subcellular level determines the outcome of bacteriophage infection. *Cell*, 141(4):682–691, 2010.
29. Maslov S and Sneppen K. Well-temperate phage: optimal bet-hedging against local environmental collapses. *Scientific Reports*, 5(1):10523, 2015.
30. Golding I. Infection by bacteriophage lambda: an evolving paradigm for cellular individuality. *Curr Opin Microbiol*, 43:9–13, 2018.
31. Li G, Cortez MH, Dushoff J, and Weitz JS. When to be temperate: on the fitness benefits of lysis vs. lysogeny. *Virus Evolution*, 6(2):veaa042, 2020.
32. Golding I, Coleman S, Nguyen TVP, and Yao T. Decision making by temperate phages. In Bamford DH and Zuckerman M, editors, *Encyclopedia of Virology (Fourth Edition)*, pages 88–97. Academic Press, Oxford, fourth edition, 2021.
33. Geng Y, Nguyen TVP, Homaee E, and Golding I. Using bacterial population dynamics to count phages and their lysogens. *Nature Communications*, 15(1):7814, 2024.
34. Goel T, Beckett SJ, and Weitz JS. Eco-evolutionary dynamics of temperate phages in periodic environments. *bioRxiv*, 2024.
35. Storms ZJ and Sauvageau D. Modeling tailed bacteriophage adsorption: Insight into mechanisms. *Virology*, 485:355–362, 2015.
36. Leprince A and Mahillon J. Phage adsorption to gram-positive bacteria. *Viruses*, 15(1):196, 2023. Article number 196.
37. Krueger AP and Northrop JH. The kinetics of the bacterium-bacteriophage reaction. *The Journal of General Physiology*, 14(2):223–254, November 1930.
38. Krueger AP. The sorption of bacteriophage by living and dead susceptible bacteria: I. equilibrium conditions. *The Journal of General Physiology*, 14(4):493–516, March 1931.
39. Delbrück M. Adsorption of bacteriophage under various physiological conditions of the host. *The Journal of General Physiology*, 23(5):631–642, May 1940.
40. Luria SE and Delbrück M. Mutations of bacteria from virus sensitivity to virus resistance. *Genetics*, 28(6):491–511, Nov 1943.
41. Weidel W. Über die zellmembran von escherichia coli b: I. präparierung der membranen. analytische daten. morphologie. verhalten der membranen gegenüber den bakteriophagen der t-serie. *Zeitschrift für Naturforschung B*, 6(5):251–259, 1951.
42. Weidel W and Kellenberger E. The e. coli b-receptor for the phage t5. ii. electron microscopic studies. *Biochimica et Biophysica Acta*, 17(1):1–9, May 1955.
43. Weidel W. Bacterial viruses; with particular reference to adsorption/penetration. *Annual Review of Microbiology*, 12:27–48, 1958.
44. Anderson TF. The reactions of bacterial viruses with their host cells. *The Botanical Review*, 15(7):464–505, 1949.
45. Garen A and Puck TT. The first two steps of the invasion of host cells by bacterial viruses. ii. *The Journal of Experimental Medicine*, 94(3):177–189, Sep 1951.
46. Stent GS and Wollman EL. On the two step nature of bacteriophage absorption. *Biochimica et Biophysica Acta*, 8(3):260–269, Mar 1952.
47. Randall-Hazelbauer L and Schwartz M. Isolation of the bacteriophage lambda receptor from escherichia coli. *Journal of Bacteriology*, 116(3):1436–1446, Dec 1973.
48. Schwartz M and Le Minor L. Occurrence of the bacteriophage λ receptor in some enterobacteriaceae. *Journal of Virology*, 15(4):679–685, 1975.
49. Schwartz M. Reversible interaction between coliphage lambda and its receptor protein. *Journal of Molecular Biology*, 99(1):185–201, 1975.
50. Szmelcman S and Hofnung M. Maltose transport in escherichia coli k-12: involvement of the bacteriophage lambda receptor. *Journal of Bacteriology*, 124(1):112–118,

1975.
51. Schwartz M. The adsorption of coliphage lambda to its host: effect of variations in the surface density of receptor and in phage-receptor affinity. *Journal of Molecular Biology*, 103(3):521–536, 1976.
52. Schwartz M. *Interaction of Phages with their Receptor Proteins*, pages 59–94. Springer Netherlands, Dordrecht, 1980.
53. Braun V, Schaller K, and Wolff H. A common receptor protein for phage t5 and colicin m in the outer membrane of escherichia coli b. *Biochimica et Biophysica Acta*, 323(1):87–97, Sep 1973.
54. Hantke K and Braun V. Membrane receptor dependent iron transport in escherichia coli. *FEBS Letters*, 49(3):301–305, January 1975.
55. Hancock RW and Braun V. Nature of the energy requirement for the irreversible adsorption of bacteriophages t1 and phi80 to escherichia coli. *Journal of Bacteriology*, 125(2):409–415, 1976.
56. Hantke K and Braun V. Functional interaction of the *tonA/tonB* receptor system in *Escherichia coli*. *Journal of Bacteriology*, 135(1):190–197, 1978.
57. Kadner RJ, Heller K, Coulton JW, and Braun V. Genetic control of hydroxamate-mediated iron uptake in *Escherichia coli*. *Journal of Bacteriology*, 143(1):256–264, 1980.
58. Schöffler H and Braun V. Transport across the outer membrane of *Escherichia coli* k12 via the fhua receptor is regulated by the tonb protein of the cytoplasmic membrane. *Molecular and General Genetics MGG*, 217(2):378–383, 1989.
59. Killmann H and Braun V. Energy-dependent receptor activities of *Escherichia coli* k-12: mutated tonb proteins alter fhua receptor activities to phages t5, t1, phi 80 and to colicin m. *FEMS Microbiology Letters*, 119(1-2):71–76, June 1994.
60. Killmann H, Videnov G, Jung G, Schwarz H, and Braun V. Identification of receptor binding sites by competitive peptide mapping: phages t1, t5, and phi 80 and colicin m bind to the gating loop of fhua. *Journal of Bacteriology*, 177(3):694–698, February 1995.
61. Killmann H, Benz R, and Braun V. Properties of the fhua channel in the *Escherichia coli* outer membrane after deletion of fhua portions within and outside the predicted gating loop. *Journal of Bacteriology*, 178(23):6913–6920, December 1996.
62. Braun V. Fhua (tona), the career of a protein. *Journal of Bacteriology*, 191(11):3431–3436, June 2009. Epub 2009 Mar 27. Review; Research Support, Non-U.S. Gov't.
63. Braun V. The outer membrane took center stage. *Annual Review of Microbiology*, 72:1–24, 2018. Autobiography; Historical Article; Portrait.
64. Brown S, Mitarai N, and Sneppen K. Protection of bacteriophage-sensitive escherichia coli by lysogens. *Proceedings of the National Academy of Sciences*, 119(14):e2106005119, 2022.
65. Winther T, Xu L, Berg-Sørensen K, Brown S, and Oddershede L. Effect of energy metabolism on protein motility in the bacterial outer membrane. *Biophysical Journal*, 97:1305–1312, 2009.
66. Nguyen TVP, Wu Y, Yao T, Trinh JT, Zeng L, Chemla YR, and Golding I. Coinfecting phages impede each other's entry into the cell. *Current Biology*, 34(13):2841–2853, 2024.
67. Schlesinger M. Adsorption of bacteriophages to homologous bacteria. ii. quantitative investigation of adsorption velocity and saturation. estimation of the particle size of the bacteriophage. *Zeitschrift für Hygiene und Infektionskrankheiten*, 114:149–160, 1932.
68. Heller K and Braun V. Accelerated adsorption of bacteriophage t5 to *Escherichia coli* f, resulting from reversible tail fiber-lipopolysaccharide binding. *Journal of Bacteriology*, 139(1):32–38, 1979.
69. Moldovan R, Chapman-McQuiston E, and Wu XL. On kinetics of phage adsorption. *Biophysical Journal*, 93(1):303–315, 2007.
70. Storms ZJ, Smith L, Sauvageau D, and Cooper DG. Modeling bacteriophage attachment using adsorption efficiency. *Biochemical Engineering Journal*, 64:22–29, 2012.
71. Tomat D, Aquili V, Casabonne C, and Quiberoni A. Influence of physicochemical factors on adsorption of ten *Shigella flexneri* phages. *Viruses*, 14(12):2815, 2022.
72. Hendrix RW and Duda RL. Bacteriophage λ papa: not the mother of all λ phages. *Science*, 258(5085):1145–1148, 1992.
73. De Paepe M and Taddei F. Viruses' life history: Towards a mechanistic basis of a trade-off between survival and reproduction among phages. *PLOS Biology*, 4(7):null, June 2006.
74. Shao Y and Wang IN. Bacteriophage adsorption rate and optimal lysis time. *Genetics*, 180(1):471–482, 2008.
75. Tzagoloff H and Pratt D. The initial steps in infection with coliphage m13. *Virology*, 24(3):372–380, 1964.
76. Ferguson AD, Hofmann E, Coulton JW, Diederichs K, and Welte W. Siderophore-mediated iron transport: crystal structure of fhua with bound lipopolysaccharide. *Science*, 282(5397):2215–2220, Dec 1998.
77. Nakae T. Outer membrane of salmonella. isolation of protein complex that produces transmembrane channels. *Journal of Biological Chemistry*, 251(7):2176–2178, Apr 1976.
78. Hantke K. Phage t6 — colicin k receptor and nucleoside transport in escherichia coli. *FEBS Letters*, 70(1):109–112, 1976.
79. Manning PA and Reeves P. Outer membrane proteins of escherichia coli k-12: Isolation of a common receptor protein for bacteriophage t6 and colicin k. *Molecular and General Genetics MGG*, 158(3):279–286, 1978.
80. Bremer E, Gerlach P, and Middendorf A. Double negative and positive control of tsx expression in escherichia coli. *Journal of Bacteriology*, 170(1):108–116, Jan 1988.
81. Bremer E, Middendorf A, Martinussen J, and Valentin-Hansen P. Analysis of the tsx gene, which encodes a nucleoside-specific channel-forming protein (tsx) in the outer membrane of escherichia coli. *Gene*, 96(1):59–65, 1990.
82. Luckey M, Wayne R, and Neilands JB. In vitro competition between ferrichrome and phage for the outer membrane t5 receptor complex of escherichia coli. *Biochemical and Biophysical Research Communications*, 64(2):687–693, May 1975.
83. Poon APW and Dhillon TS. The attachment sites of t5-host range temperate coliphages. *Virology*, 158(2):431–434, 1987.
84. Postle K. Tonb protein and energy transduction between membranes. *Journal of Bioenergetics and Biomembranes*, 25(6):591–601, 1993.

85. Postle K and Kadner RJ. Touch and go: tying tonb to transport. *Molecular Microbiology*, 49(4):869–882, 2003.
86. Postle K and Larsen RA. Tonb-dependent energy transduction between outer and cytoplasmic membranes. *Biometals*, 20(3-4):453–465, Jun 2007.
87. Lederberg EM. Lysogenicity in e-coli k-12. In *Genetics*, volume 36, pages 560–560. 428 EAST PRESTON ST, BALTIMORE, MD 21202, 1951.
88. Oddershede L, Kisbye J, Grego S, Brown S, and Berg-Sørensen K. The motion of a single protein, the λ-receptor, in the bacterial outer membrane. *Biophysical Journal*, 83:3152–3161, 2002.
89. Vidakovic L, Singh PK, Hartmann R, Nadell CD, and Drescher K. Dynamic biofilm architecture confers individual and collective mechanisms of viral protection. *Nature Microbiology*, 3(1):26–31, 2018. Epub 2017 Oct 30. PMCID: PMC5739289.
90. Pearl S, Gabay C, Kishony R, Oppenheim A, and Balaban NQ. Nongenetic individuality in the host–phage interaction. *PLoS Biology*, 6(5):e120, 2008.
91. Himeoka Y and Mitarai N. Dynamics of bacterial populations under the feast-famine cycles. *Physical Review Research*, 2(1):013372, 2020.
92. Kolter R, Balaban N, and Julou T. Bacteria grow swiftly and live thriftily. *Current Biology*, 32(12):R599–R605, 2022.
93. Mitarai N, Marantos A, and Sneppen K. Sustainable diversity of phage-bacteria systems. *Current Opinion in Systems Biology*, 35:100468, 2023.